



Non-linear Free Vibration Analysis of a Thick Sandwich Panel with an Electrorheological Core

Mehdi Keshavarzian¹ · Mohammad M. Najafizadeh¹ · Korosh Khorshidi² · Peyman Yousefi³ · Seyed Majid Alavi⁴

Received: 18 July 2021 / Revised: 28 February 2022 / Accepted: 9 March 2022 / Published online: 4 May 2022
© Krishtel eMaging Solutions Private Limited 2022

Abstract

Background Free vibrations with high amplitude behave mainly nonlinearly, which can be dangerous to structures. Thus, they must be controlled effectively. We used an improved higher-order shear deformation theory for analyzing the nonlinear versus linear vibration of a composite sandwich panel with an Electrorheological (ER) Core and examined the hardening and softening behaviors.

Methods The boundary conditions and governing equations were extracted by Hamilton's principle. Via the harmonic balance method, we solved the equation analytically with quadratic and cubic nonlinearities and the data were compared with the established results. Ordinary differential equations were yielded by applying Galerkin's approximation technique to the governing partial differential equations.

Results As each of the parameters of the aspect ratio and the sandwich panel thickness and damping increases, the vibration amplitude decreases. This means the increase of non-linear frequency by the increased amplitude. By increasing the thickness of the ER layer, the natural frequency of the structure increased. An increase was found in hardening behavior for the orthotropic and thick sandwich panel.

Conclusions By increasing the electric field in the nonlinear state, the structure hardens significantly, which improves the system's stability. To control the vibration behavior, increasing the electric field decreases the structure's frequency while increasing the panel's aspect ratio increases the frequency.

Keywords Electrorheological core · Harmonic balance · Large amplitude · Nonlinear vibration · Sandwich panel

✉ Mohammad M. Najafizadeh
m-najafizadeh@iau-arak.ac.ir
Mehdi Keshavarzian
mehdikeshavarzianme@gmail.com
Korosh Khorshidi
K-khorshidi@araku.ac.ir
Peyman Yousefi
p-yousefi@iau-arak.ac.ir
Seyed Majid Alavi
m-alavi@iau-arak.ac.ir

¹ Department of Mechanical Engineering, School of Engineering, Islamic Azad University, Arak, Iran

² Department of Mechanical Engineering, Faculty of Engineering, Arak University, Arak, Iran

³ Department of Mechanical Engineering, School of Engineering, Islamic Azad University, Arak, Iran

⁴ Department of Mathematics, Islamic Azad University, Arak, Iran

Introduction

High-strength and lightweight composites were applied effectively in numerous fields of material science engineering. The nonlinear vibration of laminated composite plates has obtained a huge deal of attention since they are suitable for use in harsh environments. To fit a variety of material applications, it is critical to determine the frequency of the nonlinear vibration accurately.

The nonlinear vibration behavior of plates was extensively assessed utilizing different approximation methods. Several authors studied the plates' nonlinear vibration behavior for laminated and isotropic composite plates.

Large deflection vibration of cross-ply laminated plates with certain edge conditions. Journal of Sound and Vibration studied by Chandra [1]. Chandra et al. analyzed Large deflection vibration of angle ply laminated plates [2]. Singh et al. investigated Non-linear vibrations of simply supported rectangular cross-ply plates. Journal of Sound and Vibration

[3]. Singh et al. presented Large amplitude free vibration of simply supported antisymmetric cross-ply plates [4]. Nonlinear vibrations of rectangular laminated composite plates with different boundary conditions. Was reviewed by Amabili et al. [5]. Analytical Nonlinear Elasto-Plastic Impact Response of a Moderately Thick Rectangular Plate has been studied by Khorshidi [6].

The Homotopy Perturbation Method (HPM) for nonlinear vibration behavior of functionally graded plates analyzed by Yazdi [7]. The HPM was further used to analyze the geometrical nonlinear vibrations of thin rectangular laminated plates made of functionally graded material (FGM). Using Von Karman's strain displacement relations, the structural nonlinearity of the system has been modeled. Quan and Duc studied Nonlinear vibration and dynamic response of shear deformable imperfect functionally graded double curved shallow shells resting on elastic foundations in thermal environments [8]. Vibration and nonlinear dynamic response of imperfect sandwich piezoelectric auxetic plate were reviewed by Quan et al. [9].

Andrianov et al. presented An artificial small perturbation parameter and nonlinear plate vibrations. *Journal of Sound and Vibration* [10]. Duc and Tung investigated Nonlinear analysis of stability for functionally graded cylindrical shells under axial compression [11]. An analytical approach for nonlinear thermo-electro-elastic forced vibration of piezoelectric penta-graphene plates has been done by Quan Quyen and Duc [12]. Differential quadrature method for nonlinear vibration of orthotropic plates with finite deformation and transverse shear effect provided by Li and Cheng [13]. These authors assessed the nonlinear free vibration behavior by the differential quadrature technique, using the harmonic balance process to derive the equations of motion. Lal et al. [14] presented Nonlinear free vibration of laminated composite plates on elastic foundation with random system properties. Typical numerical results (second-order statistics) were obtained for the composite plates resting on Winkler and Pasternak elastic foundations with different support conditions. Quan et al. presented Vibration and nonlinear dynamic response of imperfect sandwich piezoelectric auxetic plate [9]. Nonlinear buckling and postbuckling of imperfect piezoelectric S-FGM circular cylindrical shells with metal-ceramic-metal layers in thermal environment using Reddy's third-order shear deformation shell theory Was reviewed by Khoa et al. [15].

Tian et al. [16] presented A new higher-order analysis model for sandwich plates with flexible core.

The Vibration Controllability of Sandwich Structures with Smart Materials of Electrorheological Fluids and Magnetorheological Materials was explored by Kolekar et al. [17]. Nonlinear stability of eccentrically stiffened S-FGM elliptical cylindrical shells in thermal environment has been studied by Duc et al. [18]. Malekzadeh et al. [19]

investigated the dynamic response of in-plane pre-stressed sandwich panels with a viscoelastic flexible core and various boundary conditions. A Three-Layer Quasi-3D Finite Element Analysis for Smart Actuation on Sandwich Plates has been studied by Nabarrete [20]. Lv et al. presented The Dynamic Models, Control Strategies and Applications for Magnetorheological Damping Systems: A Systematic Review [21]. Duc investigated Nonlinear thermo-electro-mechanical dynamic response of shear deformable piezoelectric Sigmoid functionally graded sandwich circular cylindrical shells on elastic foundations [22]. Nonlinear analysis of stability for functionally graded cylindrical shells under axial compression has been done by Tungand and Duc [23].

For moderately thick laminated plates, applying classical theories can result in imprecise data. In anisotropic materials, a coupling exists between the stretching and bending of laminated composite plates. It is caused by overlooking the rotary inertia and shear strains effects. Hence, both the first-order shear deformation and higher-order SDT theories have been used to assess the laminated plates' nonlinear vibration behavior. Frostig [24] developed the higher-order sandwich panel theory. Malekzadeh et al. [25] introduced the enhanced higher-order sandwich plate theory using the first-order shear deformation theory to the face sheets. Most studies conducted in recent years, focused on the Vibration of a sandwich plate equipped with an electrorheological fluid core. the concepts of ER adaptive structures based on materials for the first time were introduced by Carlson [26]. Yeh and Chen investigated the dynamic stability problems of an ER sandwich beam and explained the dynamic behavior of a variety of sandwich plates (annular, orthotropic, orthotropic annular, and rotating polar orthotropic annular plates) with various thicknesses of the ER layer and electric field strength [27–32]. high-order linear vibration behavior of moderately thick sandwich panel equipped with an ER core evaluated by Keshavarzian et al. [33].

Despite the fact that wide studies have been conducted on the vibration performance of sandwich panels equipped with ER fluid cores, fewer studies have been published on the nonlinear vibration behavior of sandwich panels consisting of ER fluid cores. Therefore, there is a definite need for research to elucidate this subject further. Considering these facts, this study was designed for deriving the nonlinear equations of motion for sandwich panels with multi-layer face sheets and an ER fluid core. For this purpose, we used the first-order shear deformation theory, including rotary inertia. Our primary focus was to examine the impacts of geometric aspect ratio, electric field magnitude, and ER core layer thickness versus the sandwich panels dynamic properties in terms of Galerkin's method. These equations were decreased to some coupled nonlinear partial differential equations (PDEs) plus a compatibility equation after the introduction of a force function. This was accomplished

after establishing the validity of our study on isotropic and investigating the laminated rectangular panels, nonlinear and linear free vibration of a panel. Moreover, we studied the impacts of the system’s parameters on the nonlinear vibration frequency.

Theoretical Formulation

Basic Assumptions

The basic assumption was having a thick composite sandwich panel comprising two composite laminated face sheets and a core layer, in which the thickness of the bottom and top covers, and the core material were as follows: h_t, h_b, h_c . The proposed sandwich panel would have its length “ a ”, width “ b ” and total thickness as “ h ”. In addition, the orthogonal coordinates $(x, y, z, i = t, b, c)$ would be as represented in Fig. 1. In that model, the “ t ” index represents the upper sheet, “ b ” shows the lower sheet, and “ c ” represents the core.

Mathematical Formulations

The “ u, v and w ” of the face sheets plus the “ x, y (longitudinal) and z (thickness) axes” are stated as:

$$\begin{aligned} \epsilon_{0xx}^i &= \frac{\partial u_0^i}{\partial x} + \frac{1}{2} \left(\frac{\partial w_0^i}{\partial x} \right)^2, \epsilon_{0yy}^i = \frac{\partial v_0^i}{\partial y} + \frac{1}{2} \left(\frac{\partial w_0^i}{\partial y} \right)^2, \gamma_{0xy}^i = \frac{\partial v_0^i}{\partial x} + \frac{\partial u_0^i}{\partial y} + \frac{\partial w_0^i}{\partial x} \frac{\partial w_0^i}{\partial y} \\ \gamma_{0xz}^i &= \frac{\partial w_0^i}{\partial x}, \gamma_{0yz}^i = \frac{\partial w_0^i}{\partial y}, L_{xx}^i = \frac{\partial^2 w_0^i}{\partial x^2}, k_{xx}^i = \frac{\partial \phi_x^i}{\partial x}, L_{yy}^i = \frac{\partial^2 w_0^i}{\partial y^2}, k_{yy}^i = \frac{\partial \phi_y^i}{\partial y}, \\ L_{xy}^i &= 2 \frac{\partial^2 w_0^i}{\partial x \partial y}, k_{xy}^i = \frac{\partial \phi_x^i}{\partial y} + \frac{\partial \phi_y^i}{\partial x}, G_{xz}^i = \frac{\partial w_0^i}{\partial x}, T_{xz}^i = \phi_x^i, G_{yz}^i = \frac{\partial w_0^i}{\partial y}, T_{yz}^i = \phi_y^i. \end{aligned} \tag{3}$$

$$\begin{aligned} u_i(x, z, y, t) &= u_0^i(x, y, t) + f_1(z_i) \frac{\partial w_0(x, y, t)}{\partial x} + f_2(z_i) \phi_x^i(x, y, t) \\ v_i(x, z, y, t) &= v_0^i(x, y, t) + f_1(z_i) \frac{\partial w_0(x, y, t)}{\partial y} + f_2(z_i) \phi_y^i(x, y, t); (i = t, b) \\ w_i(x, z, y, t) &= w_0^i(x, y, t), \end{aligned} \tag{1}$$

where “ z_i ” represents the vertical coordinate of each face sheet ($i = t, b$), which was measured upward from each face sheet mid-plane. Regarding the first-order shear deformation theory, $f_1(z_i) = 0, f_2(z_i) = z_i$, the kinematic equations for the face sheets are:

$$\begin{aligned} \epsilon_{xx}^i &= \epsilon_{0xx}^i + f_1(z_i) L_{xx}^i + f_2(z_i) k_{xx}^i, \epsilon_{yy}^i \\ &= \epsilon_{0yy}^i + f_1(z_i) L_{yy}^i + f_2(z_i) k_{yy}^i, \epsilon_{zz}^i = 0, \\ \gamma_{xy}^i &= 2\epsilon_{xy}^i = \gamma_{0xy}^i + f_1(z_i) L_{xy}^i + f_2(z_i) k_{xy}^i \\ \gamma_{xz}^i &= 2\epsilon_{xz}^i = \gamma_{0xz}^i + \frac{df_1(z_i)}{dz_i} G_{xz}^i + \frac{df_2(z_i)}{dz_i} T_{xz}^i; (i = t, b) \\ \gamma_{yz}^i &= 2\epsilon_{yz}^i = \gamma_{0yz}^i + \frac{df_1(z_i)}{dz_i} G_{yz}^i + \frac{df_2(z_i)}{dz_i} T_{yz}^i \end{aligned} \tag{2}$$

where

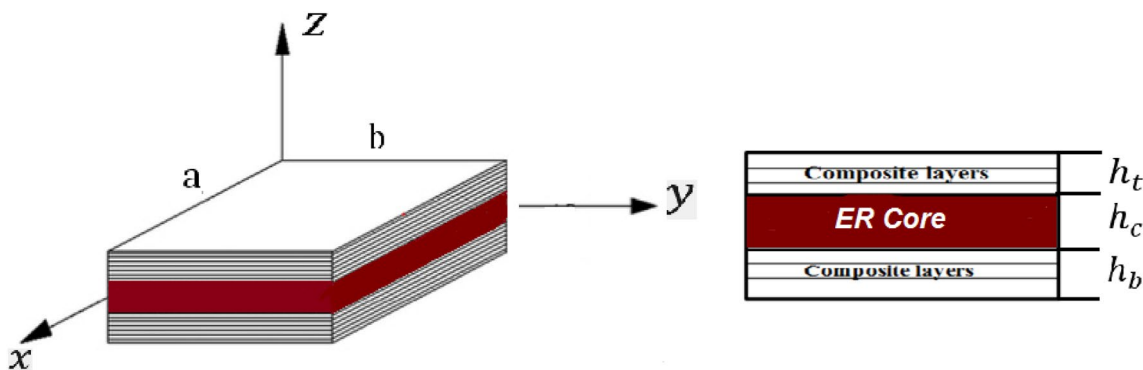


Fig. 1 A sandwich panel with laminated face sheets, an ER core and orthogonal coordinates

Displacement fields are oriented by the second Frostig’s model for the thick core layer, as follows [24]:

$$\begin{aligned}
 u_c(x, y, z, t) &= u_0^c(x, y, t) + z_c u_1^c(x, y, t) + z_c^2 u_2^c(x, y, t) + z_c^3 u_3^c(x, y, t), \\
 v_c(x, y, z, t) &= v_0^c(x, y, t) + z_c v_1^c(x, y, t) + z_c^2 v_2^c(x, y, t) + z_c^3 v_3^c(x, y, t), \\
 w_c(x, y, z, t) &= w_0^c(x, y, t) + z_c w_1^c(x, y, t) + z_c^2 w_2^c(x, y, t).
 \end{aligned}
 \tag{4}$$

The kinematic relations of the core layer are:

$$\begin{aligned}
 \epsilon_{xx}^c &= \frac{\partial u_c}{\partial x}, \epsilon_{yy}^c = \frac{\partial v_c}{\partial y}, \epsilon_{zz}^c = \frac{\partial w_c}{\partial z} \\
 \gamma_{xy}^c &= 2\epsilon_{xy}^c = \frac{\partial v_c}{\partial x} + \frac{\partial u_c}{\partial y}, \gamma_{xz}^c = 2\epsilon_{xz}^c \\
 &= \frac{\partial w_c}{\partial x} + \frac{\partial u_c}{\partial z}, \gamma_{yz}^c = 2\epsilon_{yz}^c = \frac{\partial w_c}{\partial y} + \frac{\partial v_c}{\partial z}.
 \end{aligned}
 \tag{5}$$

By placing the (4) in the relations (5) the strains in terms of the displacement of the mid-plane can be obtained as follows:

$$\begin{aligned}
 \epsilon_{xx}^c &= (\epsilon_{0xx} + z_c \chi_{0xx} + z_c^2 \epsilon_{0xx}^* + z_c^3 \chi_{0xx}^*), \\
 \epsilon_{yy}^c &= (\epsilon_{0yy} + z_c \chi_{0yy} + z_c^2 \epsilon_{0yy}^* + z_c^3 \chi_{0yy}^*) \\
 \epsilon_{zz}^c &= \epsilon_{0zz} + z_c \chi_{0zz} \\
 \gamma_{xy}^c &= \epsilon_{0xy} + z_c \chi_{0xy} + z_c^2 \epsilon_{0xy}^* + z_c^3 \chi_{0xy}^* \\
 &\quad + \epsilon_{0yx} + z_c \chi_{0yx} + z_c^2 \epsilon_{0yx}^* + z_c^3 \chi_{0yx}^* \\
 \gamma_{xz}^c &= \epsilon_{0xz} + z_c \chi_{0xz} + z_c^2 \epsilon_{0xz}^* \\
 &\quad + z_c^3 \chi_{0xz}^* + \epsilon_{1xz} + z_c \chi_{1xz} + z_c^2 \epsilon_{1xz}^* \\
 \gamma_{yz}^c &= \epsilon_{0yz} + z_c \chi_{0yz} + z_c^2 \epsilon_{0yz}^* + z_c^3 \chi_{0yz}^* \\
 &\quad + \epsilon_{1yz} + z_c \chi_{1yz} + z_c^2 \epsilon_{1yz}^*,
 \end{aligned}
 \tag{6}$$

where

$$\begin{aligned}
 \epsilon_{0xx} &= \frac{\partial u_0^c}{\partial x}, \chi_{0xx} = \frac{\partial u_1^c}{\partial x}, \epsilon_{0xx}^* = \frac{\partial u_2^c}{\partial x}, \chi_{0xx}^* = \frac{\partial u_3^c}{\partial x}, \epsilon_{0yy} = \frac{\partial v_0^c}{\partial y}, \\
 \chi_{0yy} &= \frac{\partial v_1^c}{\partial y}, \epsilon_{0yy}^* = \frac{\partial v_2^c}{\partial y}, \chi_{0yy}^* = \frac{\partial v_3^c}{\partial y}, \epsilon_{0zz} = w_0^c, \chi_{0zz} = 2w_1^c \\
 \epsilon_{0xy} &= \frac{\partial v_0^c}{\partial x}, \chi_{0xy} = \frac{\partial v_1^c}{\partial x}, \epsilon_{0xy}^* = \frac{\partial v_2^c}{\partial x}, \chi_{0xy}^* = \frac{\partial v_3^c}{\partial x}, \epsilon_{0yx} = \frac{\partial u_0^c}{\partial y}, \chi_{0yx} = \frac{\partial u_1^c}{\partial y} \\
 \epsilon_{0yx}^* &= \frac{\partial u_2^c}{\partial y}, \chi_{0yx}^* = \frac{\partial u_3^c}{\partial y}, \epsilon_{0xz} = \frac{\partial w_0^c}{\partial x}, \chi_{0xz} = \frac{\partial w_1^c}{\partial x}, \epsilon_{0xz}^* = \frac{\partial w_2^c}{\partial x}, \chi_{0xz}^* = 0 \\
 \epsilon_{1xz} &= u_1^c, \chi_{1xz} = 2u_2^c, \epsilon_{1xz}^* = 3u_3^c, \epsilon_{0yz} = \frac{\partial w_0^c}{\partial y}, \chi_{0yz} = \frac{\partial w_1^c}{\partial y}, \epsilon_{0yz}^* = \frac{\partial w_2^c}{\partial y} \\
 \chi_{0yz}^* &= 0, \epsilon_{1yz} = v_1^c, \chi_{1yz} = 2v_2^c, \epsilon_{1yz}^* = 3v_3^c.
 \end{aligned}
 \tag{7}$$

The following compatibility circumstances are obtained assuming a perfect bonding between the bottom and top face sheets and core interfaces:

$$\begin{cases} u_c(z = z_{ci}) = u_0^i + \frac{1}{2}(-1)^k h_i \phi_x^i \\ v_c(z = z_{ci}) = v_0^i + \frac{1}{2}(-1)^k h_i \phi_y^i \\ w_c(z = z_{ci}) = w_0^i \end{cases} \begin{cases} \text{For } i = t \rightarrow \left(k = 1; z_{ct} = \frac{h_c}{2} \right) \\ \text{For } i = b \rightarrow \left(k = 0; z_{cb} = -\frac{h_c}{2} \right) \end{cases}
 \tag{8}$$

Applying Eqs. (4) and (6) with some simplifications, the compatibility circumstances may be expressed as:

$$\begin{aligned}
 u_2^c &= \frac{2(u_0^t + u_0^b) - h_t \phi_x^t + h_b \phi_x^b - 4u_0^c}{h_c^2}, \\
 u_3^c &= \frac{4(u_0^t - u_0^b) - 2(h_t \phi_x^t + h_b \phi_x^b) - 4h_c u_1^c}{h_c^3} \\
 v_2^c &= \frac{2(v_0^t + v_0^b) - h_t \phi_y^t + h_b \phi_y^b - 4v_0^c}{h_c^2}, \\
 v_3^c &= \frac{4(v_0^t - v_0^b) - 2(h_t \phi_y^t + h_b \phi_y^b) - 4h_c v_1^c}{h_c^3} \\
 w_1^c &= \frac{(w_0^t + w_0^b)}{h_c}, w_2^c = \frac{2(w_0^t + w_0^b) - 4w_0^c}{h_c^2}
 \end{aligned}
 \tag{9}$$

According to Eq. (7), the number of unknown elements in the core layer is decreased to five items as: $u_0^c, u_1^c, v_0^c, v_1^c$ and w_0^c . Therefore, the unknowns for a flat composite sandwich panel consist of fifteen items as follows:

$$\left\{ u_0^t, v_0^t, w_0^t, \psi_x^t, \psi_y^t, u_0^b, v_0^b, w_0^b, \psi_x^b, \psi_y^b, u_0^c, u_1^c, v_0^c, v_1^c, w_0^c \right\}.$$

resultants of the Stress for the Core

The stress has the following results on core:

$$\begin{aligned}
 \begin{Bmatrix} N_{xx}^c \\ N_{yy}^c \\ N_{xy}^c \end{Bmatrix} &= \int_{-h_c/2}^{h_c/2} \begin{Bmatrix} \sigma_{xx}^c \\ \sigma_{yy}^c \\ \sigma_{xy}^c \end{Bmatrix} dz_c, \begin{Bmatrix} M_{nxx}^c \\ M_{nyy}^c \\ M_{nxy}^c \end{Bmatrix} \\
 &= \int_{-h_c/2}^{h_c/2} z_c^n \begin{Bmatrix} \sigma_{xx}^c \\ \sigma_{yy}^c \\ \sigma_{xy}^c \end{Bmatrix} dz_c, \begin{Bmatrix} N_{xz}^c \\ N_{yz}^c \\ M_{nxz}^c \\ M_{nyz}^c \end{Bmatrix} \\
 &= \int_{-h_c/2}^{h_c/2} z_c^n \begin{Bmatrix} \sigma_{xz}^c \\ \sigma_{yz}^c \\ z_c^n \sigma_{xz}^c \\ z_c^n \sigma_{yz}^c \end{Bmatrix} dz_c \\
 \{R_z^c, M_z^c\} &= \int_{-h_c/2}^{h_c/2} (1, z_c) \sigma_{zz}^c dz_c, \quad n = 1, 2, 3.
 \end{aligned}
 \tag{10}$$

Resulting Stress per Unit Length of the Face Sheets

resultant stress per unit length of the face sheets is defined as follows:

$$\begin{aligned}
 \begin{Bmatrix} N_{xx}^i \\ N_{yy}^i \\ N_{xy}^i \end{Bmatrix} &= \int_{-h_i/2}^{h_i/2} \begin{Bmatrix} \sigma_{xx}^i \\ \sigma_{yy}^i \\ \sigma_{xy}^i \end{Bmatrix} dz_i, \begin{Bmatrix} M_{xx}^i \\ M_{yy}^i \\ M_{xy}^i \end{Bmatrix} \\
 &= \int_{-h_i/2}^{h_i/2} f_1(z_i) \begin{Bmatrix} \sigma_{xx}^i \\ \sigma_{yy}^i \\ \sigma_{xy}^i \end{Bmatrix} dz_i, \begin{Bmatrix} P_{xx}^i \\ P_{yy}^i \\ P_{xy}^i \end{Bmatrix} \\
 &= \int_{-h_i/2}^{h_i/2} f_2(z_i) \begin{Bmatrix} \sigma_{xx}^i \\ \sigma_{yy}^i \\ \sigma_{xy}^i \end{Bmatrix} dz_i \\
 N_{xz}^i &= k_s \int_{-h_i/2}^{h_i/2} \sigma_{xz}^i dz_i, R_{xz}^i = k_s \int_{-h_i/2}^{h_i/2} \left(\frac{df_1(z_i)}{dz} \right)^i \sigma_{xz}^i dz_i, S_{xz}^i \\
 &= k_s \int_{-h_i/2}^{h_i/2} \left(\frac{df_2(z_i)}{dz} \right)^i \sigma_{xz}^i dz_i, i = t, b \\
 N_{yz}^i &= k_s \int_{-h_i/2}^{h_i/2} \sigma_{yz}^i dz_i, R_{yz}^i \\
 &= k_s \int_{-h_i/2}^{h_i/2} \left(\frac{df_1(z_i)}{dz} \right)^i \sigma_{yz}^i dz_i, S_{yz}^i \\
 &= k_s \int_{-h_i/2}^{h_i/2} \left(\frac{df_2(z_i)}{dz} \right)^i \sigma_{yz}^i dz_i, i = t, b,
 \end{aligned} \tag{11}$$

where k_s is the shear correction factor.

Equations of Motion

The Hamilton’s principle was used for extracting the sandwich panel motion equations. Analytically, the principle may be expressed as:

$$\int_0^t \delta L dt = \int_0^t (\delta K - \delta U + \delta W_{ext}) dt = 0, \tag{12}$$

where, δK and δU denote variations in the kinetic and strain energies, respectively. Also, δW_{ext} potential energy variation is caused by external forces and “ t ” is the duration

between times “ t_1 and t_2 ”, and “ δ ” represents the variation operator. Hence, the first variation equation of the kinetic energy (presuming homogeneous circumstances for velocity and displacement regarding time coordinate) is:

$$\begin{aligned}
 \delta K &= - \sum_{i=t,b,c} \left[\iint_{A_i} \int_{-h_i/2}^{h_i/2} \rho_i (\dot{u}_i \delta u_i + \dot{v}_i \delta v_i + \dot{w}_i \delta w_i) dz_i dA_i \right] \\
 dA_c &= dx_c dy_c, dA_i = dx_i dy_i, (i = t, b).
 \end{aligned} \tag{13}$$

The total strain energy stored in the sandwich panel cases and core is expressed as follows:

$$\begin{aligned}
 \delta U &= \sum_{i=t,b} \left(\int_{V_i} (\sigma_{xx}^i \delta \epsilon_{xx}^i + \sigma_{yy}^i \delta \epsilon_{yy}^i + \gamma_{xy}^i \delta \gamma_{xy}^i + \gamma_{xz}^i \delta \gamma_{xz}^i + \gamma_{yz}^i \delta \gamma_{yz}^i) dV_i \right) \\
 &+ \int_{V_c} (\sigma_{xx}^c \delta \epsilon_{xx}^c + \sigma_{yy}^c \delta \epsilon_{yy}^c + \gamma_{xy}^c \delta \gamma_{xy}^c + \gamma_{xz}^c \delta \gamma_{xz}^c + \gamma_{yz}^c \delta \gamma_{yz}^c) dV_c,
 \end{aligned} \tag{14}$$

where: $dV_c = dA_c dz_c = dx_c dy_c dz_c$, $dV_i = dA_i dz_i = dx_i dy_i dz_i$; ($i = t, b$).

Ultimately, we must substitute the relations of both the displacement fields and strain–displacement in the kinetic energy variations and system potentials. Using the Hamilton’s principle, the motion equations are obtained. Given the long equations, only one equation is given as an example:

$$\begin{aligned}
 \delta u_0^t : & \frac{\partial N_{xx}^t}{\partial x} + \frac{\partial N_{xy}^t}{\partial y} + \frac{2}{h_c^2} \frac{\partial M_{2xx}^c}{\partial x} + \frac{4}{h_c^3} \frac{\partial M_{3xy}^c}{\partial y} + \frac{2}{h_c^2} \frac{\partial M_{2xy}^c}{\partial y} - \frac{4M_{1xz}^c}{h_c^2} \\
 & - \frac{12M_{2xz}^c}{h_c^3} + \frac{4}{h_c^3} \frac{\partial M_{3xx}^c}{\partial x} = \left(-\frac{16I_5^c}{h_c^5} - \frac{8I_4^c}{h_c^4} + \frac{4I_3^c}{h_c^3} + \frac{2I_2^c}{h_c^2} \right) \\
 \ddot{u}_0^c & + \left(\frac{2I_3^c}{h_c^2} - \frac{8I_5^c}{h_c^4} - \frac{16I_6^c}{h_c^5} + \frac{4I_4^c}{h_c^3} \right) \ddot{u}_1^c + \left(\frac{4I_4^c}{h_c^4} - \frac{16I_6^c}{h_c^6} \right) \\
 \ddot{u}_0^b & + \left(\frac{16I_6^c}{h_c^6} + \frac{4I_4^c}{h_c^4} + \frac{16I_5^c}{h_c^5} + I_0^c \right) \ddot{u}_0^t + \left(\frac{2I_4^c h_b}{h_c^4} - \frac{8h_b I_6^c}{h_c^6} \right) \ddot{\phi}_x^b \\
 & + \left(-\frac{8h_t I_5^c}{h_c^5} + I_2^c - \frac{2I_4^c h_t}{h_c^4} - \frac{8h_t I_6^c}{h_c^6} \right) \ddot{\phi}_x^t + I_1^c \ddot{W}_{0,x}^t.
 \end{aligned} \tag{15}$$

The moment of inertia of the core is defined by the following equations:

$$I_n^c = \int_{-\frac{h_c}{2}}^{\frac{h_c}{2}} \rho_c z_c^n dz_c, n = 0, 1, \dots, 6 \tag{16}$$

Moreover, the moment of the face sheets inertia in relation is derived by the following equations:

$$\begin{aligned}
 I_0^t &= \int_{-\frac{h_t}{2}}^{\frac{h_t}{2}} \rho_t dz_t, I_1^t = \int_{-\frac{h_t}{2}}^{\frac{h_t}{2}} \rho_t f_1(z_i) dz_t, I_2^t \\
 &= \int_{-\frac{h_t}{2}}^{\frac{h_t}{2}} \rho_t f_2(z_i) dz_t, I_3^t = \int_{-\frac{h_t}{2}}^{\frac{h_t}{2}} \rho_t f_1(z_i) f_2(z_i) dz_t \\
 I_4^t &= \int_{-\frac{h_t}{2}}^{\frac{h_t}{2}} \rho_t [f_2(z_i)]^2 dz_t \\
 I_0^b &= \int_{-\frac{h_b}{2}}^{\frac{h_b}{2}} \rho_b dz_b, I_1^b = \int_{-\frac{h_b}{2}}^{\frac{h_b}{2}} \rho_b f_1(z_i) dz_b, I_2^b \\
 &= \int_{-\frac{h_b}{2}}^{\frac{h_b}{2}} \rho_b f_2(z_i) dz_b, I_3^b = \int_{-\frac{h_b}{2}}^{\frac{h_b}{2}} \rho_b f_1(z_i) f_2(z_i) dz_b, \\
 I_4^b &= \int_{-\frac{h_b}{2}}^{\frac{h_b}{2}} \rho_b [f_2(z_i)]^2 dz_b.
 \end{aligned} \tag{17}$$

Lamina Constitutive Relations

For *k*th orthotropic Lamina, the linear constitutive relations in the principal material coordinates are:

$$\begin{bmatrix} \sigma_{xx} \\ \sigma_{yy} \\ \sigma_{xy} \end{bmatrix} = \begin{bmatrix} Q_{11} & Q_{12} & Q_{16} \\ Q_{12} & Q_{22} & Q_{26} \\ Q_{16} & Q_{26} & Q_{66} \end{bmatrix}^{(k)} \begin{bmatrix} \epsilon_{xx} \\ \epsilon_{yy} \\ \epsilon_{xy} \end{bmatrix}, \begin{bmatrix} \sigma_{yz} \\ \sigma_{xz} \end{bmatrix} = \begin{bmatrix} Q_{44} & Q_{45} \\ Q_{45} & Q_{55} \end{bmatrix}^{(k)} \begin{bmatrix} \epsilon_{yz} \\ \epsilon_{xz} \end{bmatrix}, \tag{18}$$

where $Q_{ij}^{(k)}$ are the plane stress-reduced stiffness. For Q_{ij} of each layer, relations (19) are also available:

$$\begin{aligned}
 Q_{11} &= \frac{E_1}{1 - \nu_{12}\nu_{21}}, Q_{12} = \frac{\nu_{12}E_1}{1 - \nu_{12}\nu_{21}}, Q_{22} = \frac{E_2}{1 - \nu_{12}\nu_{21}}, \\
 Q_{66} &= G_{12}, Q_{44} = G_{23}, Q_{55} = G_{13}
 \end{aligned} \tag{19}$$

The stress–strain relations in the direction of the sandwich panel geometrical axes are derived as follows:

$$\begin{bmatrix} \sigma_{xx} \\ \sigma_{yy} \\ \sigma_{xy} \end{bmatrix} = \begin{bmatrix} \bar{Q}_{11} & \bar{Q}_{12} & \bar{Q}_{16} \\ \bar{Q}_{12} & \bar{Q}_{22} & \bar{Q}_{26} \\ \bar{Q}_{16} & \bar{Q}_{26} & \bar{Q}_{66} \end{bmatrix}^{(k)} \begin{bmatrix} \epsilon_{xx} \\ \epsilon_{yy} \\ \epsilon_{xy} \end{bmatrix}, \begin{bmatrix} \sigma_{yz} \\ \sigma_{xz} \end{bmatrix} = \begin{bmatrix} \bar{Q}_{44} & \bar{Q}_{45} \\ \bar{Q}_{45} & \bar{Q}_{55} \end{bmatrix} \begin{bmatrix} \epsilon_{yz} \\ \epsilon_{xz} \end{bmatrix}, \tag{20}$$

where, \bar{Q}_{ij} represents the transmitted stiffness in the geometrical axis of the sandwich panel.

The association between the transferred stiffness and axial stiffness is derived by the following equation:

$$\begin{aligned}
 \bar{Q}_{11} &= Q_{11} \cos^4 \theta + 2(Q_{12} + 2Q_{66}) \sin^2 \theta \cos^2 \theta + Q_{22} \sin^4 \theta \\
 \bar{Q}_{12} &= (Q_{11} + Q_{22} - 4Q_{66}) \sin^2 \theta \cos^2 \theta + Q_{12} (\sin^4 \theta + \cos^4 \theta) \\
 \bar{Q}_{22} &= Q_{11} \sin^4 \theta + 2(Q_{12} + 2Q_{66}) \sin^2 \theta \cos^2 \theta + Q_{22} \cos^4 \theta \\
 \bar{Q}_{16} &= (Q_{11} - Q_{12} - 2Q_{66}) \sin \theta \cos^3 \theta + (Q_{12} - Q_{22} + 2Q_{66}) \sin^3 \theta \cos \theta \\
 \bar{Q}_{26} &= (Q_{11} - Q_{12} - 2Q_{66}) \sin^3 \theta \cos \theta + (Q_{12} - Q_{22} + 2Q_{66}) \sin \theta \cos^3 \theta \\
 \bar{Q}_{66} &= (Q_{11} + Q_{22} - 2Q_{12} - 2Q_{66}) \sin^2 \theta \cos^2 \theta + Q_{66} (\sin^4 \theta + \cos^4 \theta) \\
 \bar{Q}_{44} &= Q_{44} \cos^4 \theta + Q_{55} \sin^4 \theta \\
 \bar{Q}_{45} &= (Q_{55} - Q_{44}) \cos \theta \sin \theta \\
 \bar{Q}_{55} &= Q_{55} \cos^4 \theta + Q_{44} \sin^4 \theta.
 \end{aligned} \tag{21}$$

By placing relation (21) in relations (11) and (10) and using relation (4), the multi-layered and thick core layer constitutive relations related to face sheets are written as follows in terms of in-plane displacements. Due to a large number of equations, the most relevant ones were placed in Appendices A, B and C.

Model of ER Material

The complex modulus of the utilized ER fluid was measured by a previous study experimentally[34] and can be stated as follows. They are called fluid types 2a and 2b, and the relations have been presented previously by [35].

$$\begin{aligned}
 G_{2a(xz)}^C &= G_{2a(xz)}^{\prime C} + iG_{2a(xz)}^{\prime\prime C}, G_{2a(yz)}^C = G_{2a(yz)}^{\prime C} + iG_{2a(yz)}^{\prime\prime C} \\
 G_{2a(xz)}^{\prime C} &= G_{2a(yz)}^{\prime C} = 15,000E^2, G_{2a(xz)}^{\prime\prime C} = G_{2a(yz)}^{\prime\prime C} = 6900,
 \end{aligned} \tag{22}$$

$$\begin{aligned}
 G_{2b(xz)}^C &= G_{2b(xz)}^{\prime C} + iG_{2b(xz)}^{\prime\prime C}, G_{2b(yz)}^C = G_{2b(yz)}^{\prime C} + iG_{2b(yz)}^{\prime\prime C} \\
 G_{2b(xz)}^{\prime C} &= G_{2b(yz)}^{\prime C} = 50,000E^2, G_{2b(xz)}^{\prime\prime C} = G_{2b(yz)}^{\prime\prime C} = 2600E + 1700,
 \end{aligned} \tag{23}$$

no normal stress exists in the ER layer and there exist only transverse shear stresses as follows:

$$\begin{aligned}
 \sigma_{xz}^c &= G_{2b(xz)}^C \gamma_{xz}^c = G_{2b(xz)}^C \left[\frac{\partial w_0^C}{\partial x} + z \frac{\partial w_1^C}{\partial x} + z^2 \frac{\partial w_2^C}{\partial x} \right] \\
 &+ G_{2b(xz)}^C [u_1^c + 2zu_2^c + 3z^2u_3^c],
 \end{aligned} \tag{24}$$

$$\begin{aligned}
 \sigma_{yz}^c &= G_{2b(yz)}^C \gamma_{yz}^c = G_{2b(yz)}^C \left[\frac{\partial w_0^C}{\partial y} + z \frac{\partial w_1^C}{\partial y} + z^2 \frac{\partial w_2^C}{\partial y} \right] \\
 &+ G_{2b(yz)}^C [v_1^c + 2zv_2^c + 3z^2v_3^c].
 \end{aligned} \tag{25}$$

The assumed responses of the relationship satisfy simply supported boundary conditions, as shown by the following relations:

$$\begin{bmatrix} u_0^j(x, y, t) \\ v_0^j(x, y, t) \\ w_0^j(x, y, t) \\ \phi_x^j(x, y, t) \\ \phi_y^j(x, y, t) \\ u_k^c(x, y, t) \\ v_k^c(x, y, t) \\ w_0^c(x, y, t) \end{bmatrix} = \sum_{n=1}^{\infty} \sum_{m=1}^{\infty} \begin{bmatrix} U_{0mn}^j \cos(\alpha_m x) \sin(\beta_n y) \\ V_{0mn}^j \sin(\alpha_m x) \cos(\beta_n y) \\ W_{0mn}^j \sin(\alpha_m x) \sin(\beta_n y) \\ \phi_{xmn}^j \cos(\alpha_m x) \sin(\beta_n y) \\ \phi_{ymn}^j \sin(\alpha_m x) \cos(\beta_n y) \\ U_{kmn}^c \cos(\alpha_m x) \sin(\beta_n y) \\ V_{kmn}^c \sin(\alpha_m x) \cos(\beta_n y) \\ W_{lmn}^j \sin(\alpha_m x) \sin(\beta_n y) \end{bmatrix} e^{i\omega t}, \quad (26)$$

($k = 0, 1, 2, 3$), ($l = 0, 1, 2$),

where $\alpha_m = \frac{m\pi}{a}$ and $\beta_n = \frac{n\pi}{b}$

In Eq. (26), $U_{0mn}^j, V_{0mn}^j, W_{0mn}^j, \phi_{xmn}^j, \phi_{ymn}^j, U_{kmn}^c, V_{kmn}^c$ and W_{lmn}^j , represent the Fourier coefficients while “ m ” and “ n ” representing half wave numbers along “ x ” and “ y ” directions, respectively. The nonlinear ordinary-differential equation may be obtained by substituting Eq. (26) into equations of motion, in displacement terms and applying Galerkin’s process. To solve these equations of motion of nonlinear ordinary differential, each of the equations of motion can be obtained according to one of the unknowns:

$$\left\{ u_0^t, v_0^t, w_0^t, \psi_x^t, \psi_y^t, u_0^b, v_0^b, w_0^b, \psi_x^b, \psi_y^b, u_0^c, v_0^c, w_0^c, \psi_x^c, \psi_y^c \right\}.$$

Given that transverse oscillations are considered in this paper, all time-dependent variables of relations (26) are obtained using the equation of motion, in terms of $w(t)$. the nonlinear equation of motion can be obtained symbolically as:

$$\ddot{w}(t) + \omega_L^2 w(t) + \alpha_2 w(t)^2 + \alpha_3 w(t)^3 = 0. \quad (27)$$

In the above relation, ω_L is the natural linear frequency, α_2 and α_3 coefficient of nonlinear stiffness.

Solving the Equation of Motion

The obtained nonlinear equation of motion (27) can be solved, using perturbation techniques including the harmonic balance method as described by a previous study [36].

Hardening/Softening Behavior in Nonlinear Oscillations

According to the same study [36], the effective nonlinearity coefficient δ is obtained by:

$$\delta = \frac{10a_2^2 - 9a_3\omega_L^2}{24\omega_L^2}. \quad (28)$$

Hence, “ δ ” represents the extent of the resonance curves bending. When the value of $\delta > 0$, the frequency response curves are declined to the right where the type of effective nonlinearity becomes hardening. Conversely, when the value of $\delta < 0$, the frequency–response curves are bent to the left and the effective nonlinearity becomes a softening type. Also, when $\delta = 0$, the frequency–response curves are not bent to either right or left and, by the second approximation, the system’s response becomes linear in nature.

Considering Eq. (28), it follows that the quadratic nonlinearity possesses a softening effect. When a_3 is positive, the effective nonlinearity “ δ ” may be negative or positive, based on the relative magnitudes of “ a_2 ” and “ a_3 ”.

Table 1 First dimensionless period of the flat square panel with $H = h/a = \text{variable}$, $a = b = 1$, $m, n = 1$ ($T_N = \bar{T}_N(E/p)^{1/2}/a$)

Present Model (FSDT-harmonic balance method)												
1/H				T_N Amplitude ratio								
	0.1	0.2		0.4	0.6	0.8	1.0	1.5	2.0	2.5		3.0
10	10.79	10.52		9.60	8.49	7.44	6.52	4.86	3.81	3.12	2.63	
20	21.46	20.92		19.10	16.89	14.79	12.97	9.66	7.59	6.21	5.24	
30	32.16	31.35		28.62	25.32	22.17	32.16	14.48	11.37	9.30	7.85	
40	42.87	41.79		38.14	33.75	29.55	25.91	19.31	15.16	12.40	10.47	
(FSDT- Runge -Kutta numerical integration method) [37]												
1/H				T_N Amplitude ratio								
	0.1	0.2		0.4	0.6	0.8	1.0	1.5	2.0	2.5		3.0
10	10.84	10.65		10.00	9.14	8.25	7.42	5.76	4.62	3.83	3.26	10.90
20	21.11	20.76		19.53	17.91	16.20	14.59	11.37	9.13	7.56	6.44	21.229
30	31.51	30.99		29.17	26.75	24.21	21.82	17.01	13.67	11.33	9.64	31.684
40	41.93	41.25		38.83	35.62	32.25	29.07	22.66	18.22	15.11	12.85	42.170

T_N : Non-linear period with FSDT (non-dimensional)- T_L : linear period with FSDT (non-dimensional)

Results and Discussion

Validation of the Equations

The following examples justify our research approach.

Example 1 The non-linear free vibration analysis of a flat rectangular panel with SSSS B.C.

In this case, a flat square panel without a core was considered, for which the findings of the present study were compared with those of another work. Please review the details described by Ref. [37]. References [37, 38] the components of the nonlinear strains are taken on the basis proposed by two old studies. The Geometry and mechanical properties of a square panel are selected based on the following definitions:

$$a = 1, b = 1, h = a/10, E_1 = E_2 = E_3 = 322.2 \text{ GPa},$$

$$G_{12} = G_{13} = G_{23} = E/2(1 + \nu), \nu = 0.32, \rho = 2370 \text{ Kg/m}^3.$$

As shown in Table 1, the results of the current theory with harmonic balance and von Karman’s nonlinear strains methods were compared with those obtained from the first order and nonlinear strains, described previously by Ref. [38]. Our results were also in good consistency with those reported by an older study [37].

Example 2 Nonlinear Free vibration analysis of laminated panel via SSSS B.C.

Table 2 Comparison of the frequency ratio of laminated composite square panel with SSSS boundary condition, $ab=1, h_c/h_t=1, m, n=1, alh=10$

$A_R = w_{\max}/h$ Amplitude of vibration/h	ω_{NL}/ω_L Present model (IHSDT)	ω_{NL}/ω_L [4]	ω_{NL}/ω_L [14]	ω_{NL}/ω_L [39]
0.3	1.0673	1.0796	1.0731	1.0988
0.6	1.2479	1.2867	1.2859	1.3622
0.9	1.5013	1.5691	1.5650	1.7377
1.2	1.7970	1.8779	1.8750	2.1614
1.5	2.1174	2.2414	2.2400	2.6025

Table 3 Mechanical and geometrical properties of the composite sandwich panel with multi-layer face sheets and an ER core

Geometry	Laminate face sheets	ER core
$a=0.4 \text{ m}$ $b=0.4 \text{ m}$	$\rho = 2700 \text{ kg/m}^3$ $E_1=E_2=E_3=70 \text{ GPa}$	$\rho = 1700 \text{ kg/m}^3$ $G_{2b(xz)}^C = G_{b(xz)}^{\prime C} + G_{b(xz)}^{\prime\prime C}$ $G_{2b(yz)}^C = G_{b(yz)}^{\prime C} + G_{b(yz)}^{\prime\prime C}$
$h_c = 0.5\text{mm}$ $h_t=h_b=0.5 \text{ mm}$	$G_{12} = G_{13}=G_{23}=26.9 \text{ GPa}$ $\nu = 0.3$	$G_{b(xz)}^{\prime C} = G_{b(yz)}^{\prime C} = 50000E^2$ $G_{b(xz)}^{\prime\prime C} = G_{b(yz)}^{\prime\prime C} = 2600E + 1700$

Since there was no available literature for validating the results of the current study, we had to reduce the core thickness to zero and compare the data with those reported by other references. In this case, we considered a flat sandwich panel with multi-layer face sheets and an ER core under simply supported boundary conditions (SSSS) via First-order shear deformation theory for the face sheets. For face sheets, the lay-up sequences were [90/0/core/0/90] and the sandwich panel was symmetrical about the mid-plane. The following material properties were used for computation:

$$E_1 = 412\text{GPa}, E_2 = E_3 = 10.3\text{GPa}, G_{12} = G_{13} = 6.18\text{GPa},$$

$$G_{23} = 5015\text{GPa}, \nu_{12} = 0.25, \rho = 1 \frac{\text{Kg}}{\text{m}^3}.$$

As deduced from Table 2, it may be found that our results are reasonably in good consistency with those reported by previous studies [4, 14, 39]. Table 2 shows the results of the current investigation for a flat sandwich panel with ER core utilizing the revised high-order theory of sandwich panel, as well as comparisons with results from older multilayer sheet theories. As can be shown, the current theory was able to forecast lower frequency ratios with a small error margin.

Influence of Hardening/Softening Behavior in Nonlinear Vibrations

The mechanical features of the face sheets for the ER core are shown in Table 3. Based on the data presented in Table 4, the hardening effects were much greater than the softening effects.

Nonlinear Free Vibration Analysis

The effects of altering the electric field intensity and the thickness of the ER layer were also assessed on the nonlinear frequencies of the sheets. The sandwich panel was symmetrical around the mid-plane and the lay-up sequences for face sheets were [0/0/0/core/0/0/0]. Table 5 presents the comparison of the nonlinear frequency ratios for the first vibration modes of a square sandwich panel with ER core, based on first-order shear deformation theory.

Table 4 The Values of a_3 and a_2 for flat sandwich panel with aluminum face sheet and ER core based on first shear Deformation theory

Electric field strengths	Effective nonlinearity coefficient	
$E=3.5$ kV/mm	$a_2=4.0991 \times 10^{-10}$	$a_3=4.6694 \times 10^{10}$

The lay-up sequences for face sheets were [0/0/0/core/0/0/0] and $E=3.5$ kV/mm, $a/b=1$, $h_c/h_t=1$, $m, n=1$

Comparison of Linear and Nonlinear Frequency of Flat Sandwich Panel with an ER Core

Table 5 Comparison of nonlinear frequency ratios for the first vibration modes of a square sandwich panel with ER core based on first-order shear deformation theory

$A_R = w_{max}/h$	h_c/h_t	a/b	E=0 kV/mm		E=1 kV/mm		E=2 kV/mm		E=3.5 kV/mm	
			ω_{NL}/ω_L	η_{NL}	ω_{NL}/ω_L	η_{NL}	ω_{NL}/ω_L	η_{NL}	ω_{NL}/ω_L	η_{NL}
0.1	1	1	1.0555	0.0135	1.0377	0.0250	1.0207	0.0157	1.0111	0.0079
		2	1.0630	0.0048	1.0528	0.0126	1.0363	0.0103	1.0210	0.0075
	4	1	1.0898	0.0013	1.0715	0.0041	1.0617	0.0056	1.0454	0.0047
		2	1.2076	0.0175	1.2113	0.0297	1.0553	0.0223	1.0236	0.0126
		4	1.2333	0.0065	1.1816	0.0146	1.1101	0.0152	1.0542	0.0109
0.2	1	1	1.2763	0.0017	1.2552	0.0046	1.2080	0.0063	1.1387	0.0070
		2	1.2076	0.0103	1.1439	0.0206	1.0806	0.0140	1.0440	0.0074
	4	1	1.2332	0.0036	1.1976	0.0097	1.1385	0.0086	1.0819	0.0067
		2	1.2762	0.0009	1.2623	0.0030	1.2287	0.0042	1.1715	0.0037
		4	1.6836	0.0090	1.4246	0.0184	1.2061	0.0171	1.0915	0.0111
0.4	1	1	1.7563	0.0032	1.6079	0.0079	1.3889	0.0097	1.2021	0.0083
		2	1.8751	0.00081	1.8192	0.0022	1.5312	0.0032	1.4784	0.0042
	4	1	1.6835	0.0053	1.4462	0.0120	1.2829	0.0097	1.1664	0.0060
		2	1.7562	0.0017	1.6548	0.0051	1.4783	0.0051	1.2970	0.0046
		4	1.8748	0.0004	1.8369	0.0014	1.7433	0.0021	1.5781	0.0020
0.6	1	1	2.8877	0.0030	2.2623	0.0072	1.6791	0.0088	1.3290	0.0075
		2	3.0560	0.0010	2.7097	0.0027	2.1718	0.0039	1.6676	0.0043
	4	1	3.3262	0.00025	3.1951	0.00071	2.8888	0.0011	2.3964	0.0015
		2	2.2645	0.0029	1.8617	0.0071	1.5847	0.0065	1.3459	0.0045
		4	2.3854	0.0009	2.2163	0.0028	1.9151	0.0030	1.5923	0.0031
0.8	1	1	2.5805	0.0002	2.5185	0.0007	2.3633	0.0011	2.0866	0.0011
		2	5.1779	0.0014	3.2041	0.0036	2.2570	0.0048	1.6506	0.0048
	4	1	4.4456	0.0005	3.9078	0.0013	3.0599	0.0020	2.2376	0.0024
		2	4.8625	0.00012	4.6604	0.00033	4.1865	0.00052	3.4163	0.00078
		4	2.8877	0.0018	2.4373	0.0045	1.9201	0.0044	1.5629	0.0033
1	1	1	3.0559	0.0005	2.8204	0.0017	2.3963	0.0019	1.9313	0.0021
		2	2.9245	0.00014	3.2401	0.00045	3.0260	0.00069	2.6387	0.0007
	4	1	5.8098	0.0008	4.1802	0.0021	2.8773	0.0030	2.0165	0.0032
		2	5.8615	0.00028	5.1352	0.00077	4.6835	0.0011	2.8502	0.0014
		4	6.4230	0.00006	6.1510	0.00019	5.5120	0.00030	4.4689	0.00045

The lay-up sequences for face sheets were [0/0/0/core/0/0/0] and $E=$ variable, $a/h=10$

Figure 2, shows the effect of electric field intensity on the nonlinear frequency. Figure 3 represents the variations in the modal loss factor as a function of electric field intensity.

Influence of the Core Thickness Ratio to Total Sheet Thickness on the First Natural Frequency

As reflected in Fig. 4, the nonlinear frequency increases by increasing the ratio of core thickness relative to the total sheet thickness. However, an earlier study [33] suggests that increases in the ratio of core thickness to total sheet thickness reduce the natural frequency of the sheet. Regarding the

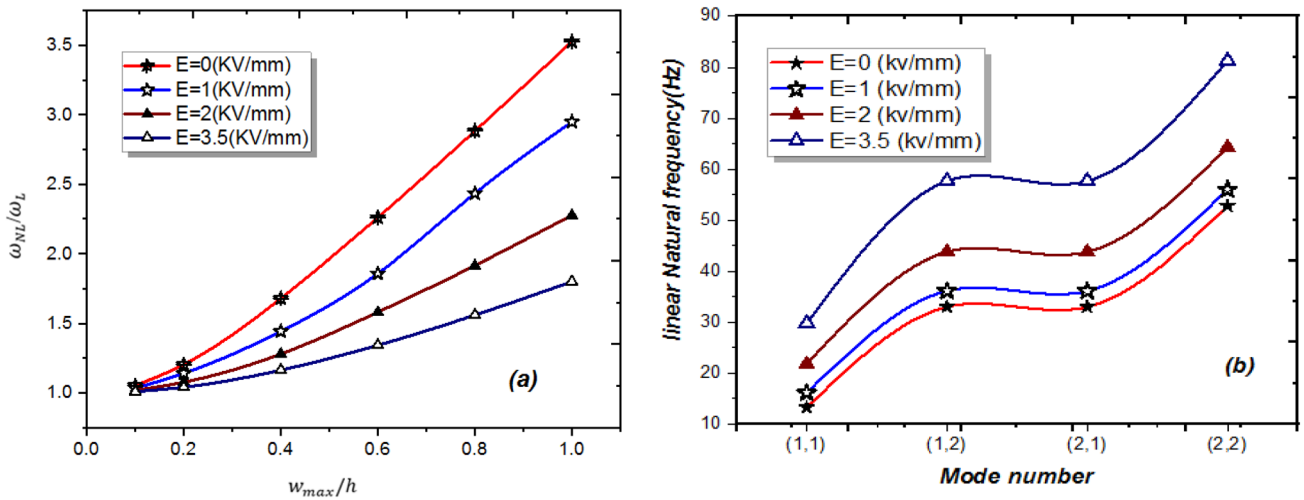


Fig. 2 Diagrammatic changes in the a nonlinear and b linear frequency of the sheet for different electric field intensities

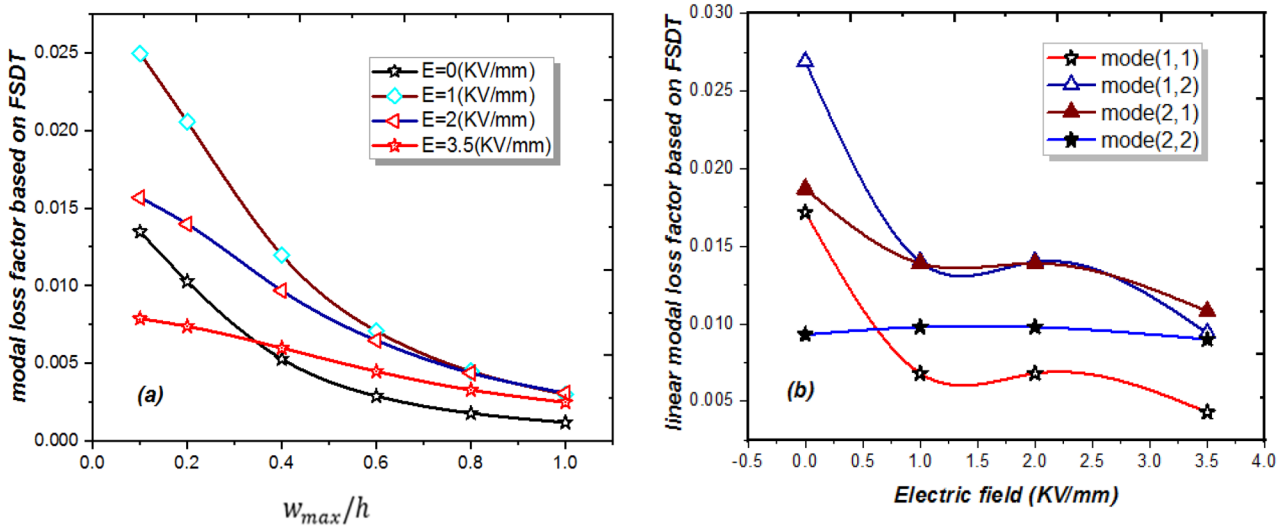


Fig. 3 Comparison of the damping coefficient in terms of vibrational modes and different electric fields for a nonlinear and b linear frequency of the sheet for different electric field intensities

nonlinear vibration, increases in the ER core thickness the ratio of the natural nonlinear frequency to the linear counterpart increases initially, then progressively declines.

Effect of Electric Field Intensity on the Nonlinear Frequency

Figure 5 illustrates the diagrammatic variations in the first nonlinear frequency of the flat sandwich panel with the ER core relative to the electric field intensity for varying aspect ratio coefficients.

Effect of Length-to-Thickness Ratio on the Natural Frequency

Figure 6 illustrates the diagram of the nonlinear frequency ratio variations of the first flat sandwich panel with an ER core based on the length to thickness ratio ($h_c/h_t = 1$, $a/b = 1$, $E = 2$ kVmm⁻¹).

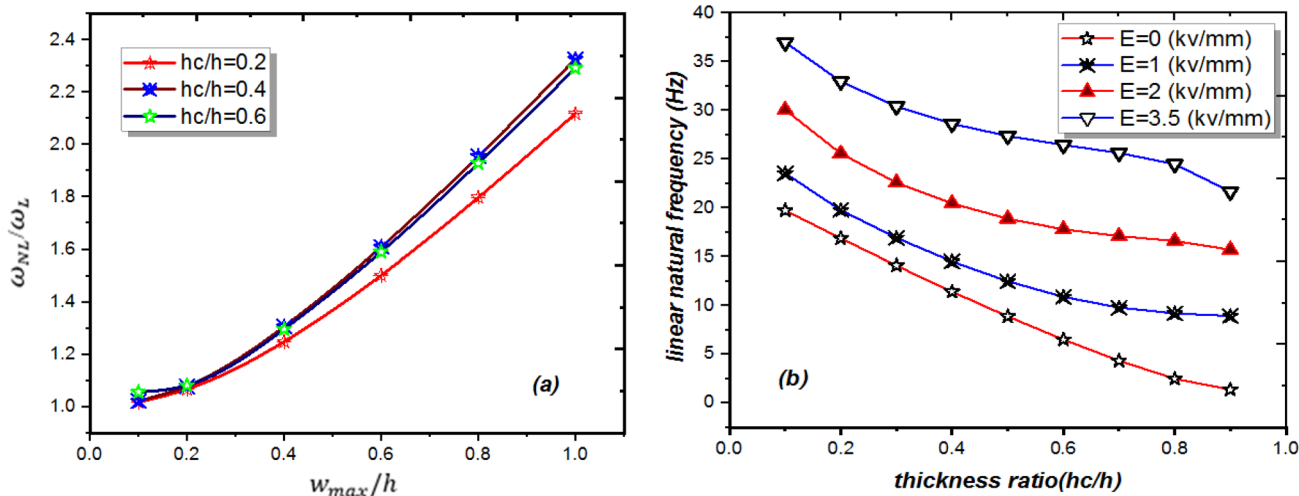


Fig. 4 Diagrams of the **a** first nonlinear ($E=2$ kV/mm) and **b** linear frequency changes of the sheet in different ratios of the core to sheet thickness, for electric field intensities

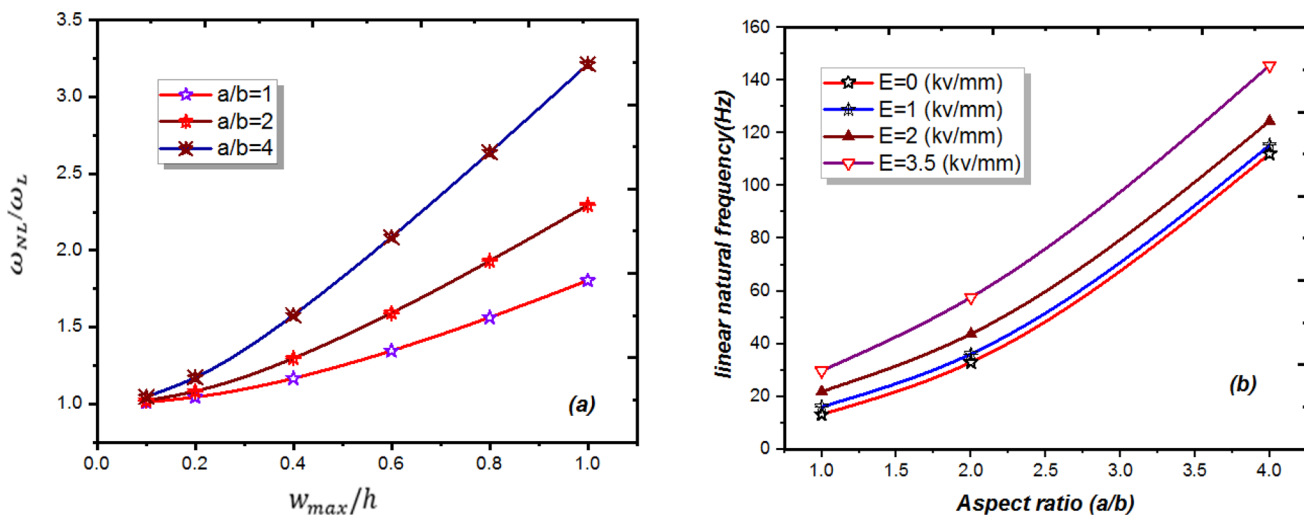


Fig. 5 Diagram of the **a** nonlinear ($E=2$ kV/mm) and **b** linear frequency ratio variations of the sheet versus the electric field intensity for different aspect ratios

Highlights

To Control the Sandwich Panel’s Nonlinear Vibration Behavior

- By increasing the electric field intensity, the nonlinear frequency of the panel decreases.
- By increasing the aspect ratio, the nonlinear frequency of the panel increases.
- By increasing the length-to-thickness ratio, the nonlinear frequency decreases.

- During the rise in the electric field intensity, if damping is applied, the vibration amplitude declines consistently.
- With an increase in the panel’s ratio, it becomes thinner while the vibration amplitude gradually increases.
- Within the ER core, the ratio of nonlinear to linear frequency increases initially, then declines consistent with increases in the core thickness.
- As the sandwich panel’s thickness grows, the hardening behavior also rises.

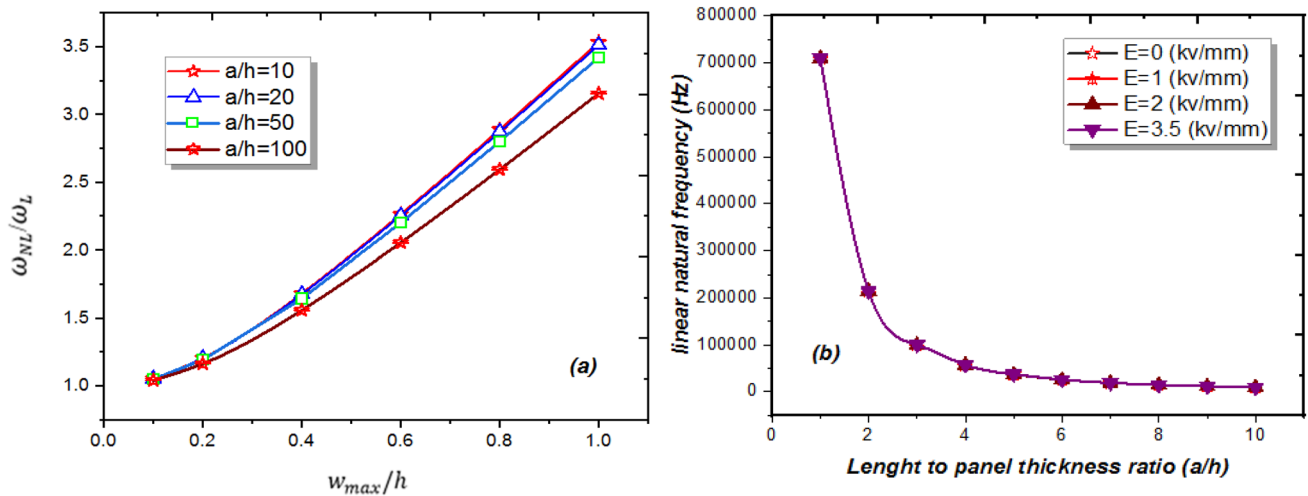


Fig. 6 The diagram of the(a) nonlinear ($E=2$ kV/mm) and (b) linear frequency ratio variations of the sheet in terms of electric field intensity for different length to thickness ratios

Conclusions

This study was undertaken for the first time to investigate the nonlinear vibration behaviors of sandwich panel with multi-layer face sheets and an ER fluid core, using an improved first-order shear deformation theory. Based on the findings, the following conclusions can be drawn:

1. With an increase in the electric field intensity, the non-linear vibration frequency of the panel decreases and the structure hardens, leading to improvement in the structure’s stability.
2. With increased damping simultaneously with a rise in the electric field intensity, the vibration amplitude declines significantly.
3. The findings enable us to develop a controllable electric field, thereby controlling the natural frequency and amplitude of the vibration in structures.
4. The contribution of the core thickness is such that by increasing it relative to the panel’s thickness at a fixed electric field intensity, the ratio of nonlinear to linear vibration frequency initially rises, then declines over time.
5. As the ratio of core thickness to that of the whole panel increases, the panel’s stiffness declines.
6. By injecting more oil into the core layer, the panel’s weight increases, thereby reducing the ratio of the panel’s density to its stiffness.
7. With an increase in the panel’s dimensional ratio, it becomes thinner while the vibration amplitude gradually increases.

8. By adjusting the above parameters, it is possible to achieve the optimal and desired nonlinear vibration frequency and amplitude in a variety of structures.

Appendix A: Descriptions of Notations

dV_p, dV_c, dV_b	The core Volume element of the top face sheet, the core and the bottom face sheet, respectively
$I_n^i (i = t, b, c)$	The moments of inertia of the top and bottom face sheets and the core
M_z^c	Normal bending moments per unit length of the edge of the core
$M_{xy}^i, M_{xx}^i, M_{yy}^i$	Bending and shear moments per unit length of the edge ($i = t, b$)
$M_{nxx}^c, M_{nxy}^c, M_{nyy}^c$	Shear and bending moments per unit length of the edge of the core, M_{nxx}^c, M_{nyy}^c
$N_{xy}^i, N_{yx}^i, N_{xx}^i, N_{yy}^i$	In-plane and shear forces per unit length of the edge ($i = t, b$)
N_{xz}^c, N_{yz}^c	Shear forces per unit length of the edge of the core
Q_{ij}	The reduced stiffnesses referred to the principal material coordinates
\bar{Q}_{ij}	Transformed reduced stiffnesses
u_k, v_k, w_k	Unknowns of the in-plane displacements of the core ($k=0,1,2,3$)
u_c, v_c, w_c	Displacement components of the core
u_0^i, v_0^i, w_0^i	Displacement components of the face sheets, ($i = t, b$)
$\ddot{u}_c, \ddot{v}_c, \ddot{w}_c$	Acceleration components of the core

$\ddot{u}_i, \ddot{v}_i, \ddot{w}_i$ Acceleration components of the face sheets, ($i=t, b$)
 Z_t, Z_b, Z_c Normal coordinates in the mid-plane of the top and the bottom face sheets and

Greek Letters

ρ_t, ρ_b, ρ_c Material densities of the face sheets and the core
 σ_{ii}^j Normal stress in the face sheets, ($i=x,y$), ($j=t,b$)
 σ_{ii}^c Normal stress in the core, ($i=x,y,z$)
 $\sigma_{xy}^i, \sigma_{xz}^j, \sigma_{yz}^i$ Shear stress in the face sheets, ($j=t,b$)
 $\sigma_{xy}^c, \sigma_{xz}^c, \sigma_{yz}^c$ Shear stresses in the core
 $\epsilon_{0xx}^i, \epsilon_{0xy}^j, \epsilon_{0yy}^k, \epsilon_{0xz}^l, \epsilon_{0xz}^j$ The mid-plane strain components, ($i=t,b$)
 $\epsilon_{zz}^c, \epsilon_{xx}^c, \epsilon_{yy}^c$ Normal strains components of the core layer
 $\gamma_{xz}^c, \gamma_{yz}^c, \gamma_{xy}^c$ Shear strains components of the core layer
 ϕ_x^i, ϕ_y^i Rotation of the normal section of midsurface of the top face sheet and the core bottom face sheet along x and y, respectively($i=t,b$)

Appendix B: Constitutive Equations for In-plane Stress Resultants

$$N_{xx}^i = A_{11}^i \left(\frac{\partial u_0^i}{\partial x} + \frac{1}{2} \left(\frac{\partial w_0^i}{\partial x} \right)^2 \right) + B_{11}^i \frac{\partial^2 w_0^i}{\partial x^2} + D_{11}^i \frac{\partial \phi_x^i}{\partial x} + A_{12}^i \left(\frac{\partial v_0^i}{\partial y} + \frac{1}{2} \left(\frac{\partial w_0^i}{\partial y} \right)^2 \right) + B_{12}^i \frac{\partial^2 w_0^i}{\partial y^2} + D_{12}^i \frac{\partial \phi_y^i}{\partial y} + A_{16}^i \left(\frac{\partial u_0^i}{\partial y} + \frac{\partial v_0^i}{\partial x} + \frac{\partial w_0^i}{\partial x} \frac{\partial w_0^i}{\partial y} \right) + B_{16}^i \left(2 \frac{\partial^2 w_0^i}{\partial x \partial y} \right) + D_{16}^i \left(\frac{\partial \phi_x^i}{\partial y} + \frac{\partial \phi_y^i}{\partial x} \right),$$

$$P_{xx}^i = E_{11}^i \left(\frac{\partial u_0^i}{\partial x} + \frac{1}{2} \left(\frac{\partial w_0^i}{\partial x} \right)^2 \right) + G_{11}^i \frac{\partial^2 w_0^i}{\partial x^2} + H_{11}^i \frac{\partial \phi_x^i}{\partial x} + E_{12}^i \left(\frac{\partial v_0^i}{\partial y} + \frac{1}{2} \left(\frac{\partial w_0^i}{\partial y} \right)^2 \right) + G_{12}^i \frac{\partial^2 w_0^i}{\partial y^2} + H_{12}^i \frac{\partial \phi_y^i}{\partial y} + E_{16}^i \left(\frac{\partial u_0^i}{\partial y} + \frac{\partial v_0^i}{\partial x} + \frac{\partial w_0^i}{\partial x} \frac{\partial w_0^i}{\partial y} \right) + G_{16}^i \left(2 \frac{\partial^2 w_0^i}{\partial x \partial y} \right) + H_{16}^i \left(\frac{\partial \phi_x^i}{\partial y} + \frac{\partial \phi_y^i}{\partial x} \right)$$

$$S_{yz}^i = K_S \left[J_{44}^i \left(\frac{\partial w_0^i}{\partial y} \right) + G_{44}^i \frac{\partial w_0^i}{\partial y} + H_{44}^i \phi_y^i + A_{45}^i \left(\frac{\partial w_0^i}{\partial x} \right) + G_{45}^i \frac{\partial w_0^i}{\partial x} + H_{45}^i \phi_x^i \right].$$

In the above equations, the stiffness coefficients for multilayer sheets are defined as follows:

$$\int_{-\frac{h_i}{2}}^{\frac{h_i}{2}} \bar{Q}_{11} dZ_i = A_{11}^i \int_{-\frac{h_i}{2}}^{\frac{h_i}{2}} \bar{Q}_{11} f_1(z_i) dZ_i = B_{11}^i \int_{-\frac{h_i}{2}}^{\frac{h_i}{2}} \bar{Q}_{11} f_2(z_i) dZ_i = D_{11}^i \int_{-\frac{h_i}{2}}^{\frac{h_i}{2}} \bar{Q}_{11} f_1(z_i) dZ_i = B_{11}^i \int_{-\frac{h_i}{2}}^{\frac{h_i}{2}} \bar{Q}_{11} f_1(z_i) f_1(z_i) dZ_i = F_{11}^i \int_{-\frac{h_i}{2}}^{\frac{h_i}{2}} \bar{Q}_{11} f_2(z_i) f_1(z_i) dZ_i = G_{11}^i \int_{-\frac{h_i}{2}}^{\frac{h_i}{2}} \bar{Q}_{12} f_2(z_i) dZ_i = E_{12}^i \int_{-\frac{h_i}{2}}^{\frac{h_i}{2}} \bar{Q}_{12} f_2(z_i) f_1(z_i) dZ_i = G_{12}^i \int_{-\frac{h_i}{2}}^{\frac{h_i}{2}} \bar{Q}_{12} f_2(z_i) f_2(z_i) dZ_i = H_{12}^i.$$

Appendix C: Constitutive Equations for the thick core layer

To define the motion equations in terms of displacement, and to facilitate solving the motion equations, the following integrals are applied:

$$e_n^{c(xx)} = \int_{-\frac{h_c}{2}}^{\frac{h_c}{2}} Z_c E_{xx}^C(Z) dz, e_n^{c(yy)} = \int_{-\frac{h_c}{2}}^{\frac{h_c}{2}} Z_c E_{yy}^C(Z) dz, g_n^{c(xy)} = \int_{-\frac{h_c}{2}}^{\frac{h_c}{2}} Z_c G_{xy}^C(Z) dz, n = 0, 1, 2, 3, g_n^{c(xz)} = \int_{-\frac{h_c}{2}}^{\frac{h_c}{2}} Z_c^n G_{(xz)}^C(Z) dz, g_n^{c(yz)} = \int_{-\frac{h_c}{2}}^{\frac{h_c}{2}} Z_c^n G_{(yz)}^C(Z) dz, n = 0, 1, 2.$$

By applying the above equations to the fundamental tension equations of the core, they can be written as follows:

$$N_{xx}^c = e_0^{c(xx)} \frac{\partial u_0^c}{\partial x} + e_1^{c(xx)} \frac{\partial u_1^c}{\partial x} + e_2^{c(xx)} \frac{\partial u_2^c}{\partial x} + e_3^{c(xx)} \frac{\partial u_3^c}{\partial x}$$

$$M_{nxx}^c = e_n^{c(xx)} \frac{\partial u_0^c}{\partial x} + e_{n+1}^{c(xx)} \frac{\partial u_1^c}{\partial x} + e_{n+2}^{c(xx)} \frac{\partial u_2^c}{\partial x} + e_{n+3}^{c(xx)} \frac{\partial u_3^c}{\partial x}$$

$$R_z^c = e_0^{c(xz)} w_1^C + 2e_1^{c(xz)} w_2^C$$

$$M_z^c = e_1^{c(xz)} w_1^C + 2g_2^{c(xz)} w_2^C$$

Acknowledgements The authors are thankful to the academic management and staff of the Department of Mechanical Engineering, School of Engineering, Islamic Azad University, Arak, Iran, for their support of this study, which was part of the doctoral thesis of the first author.

Funding This research did not receive any specific grant from funding agencies in the public, commercial, or not-for-profit sectors.

Declarations

Conflict of Interests The authors declare no conflict of interests with any internal or external entity in conducting this research.

References

- Chandra R (1976) Large deflection vibration of cross-ply laminated plates with certain edge conditions. *J Sound Vib* 47(4):509–514
- Chandra R, Raju BB (1975) Large deflection vibration of angle ply laminated plates. *J Sound Vib* 40(3):393–408
- Singh G et al (1990) Non-linear vibrations of simply supported rectangular cross-ply plates. *J Sound Vib* 142(2):213–226
- Singh G, Rao GV, Lyengar N (1991) Large amplitude free vibration of simply supported antisymmetric cross-ply plates. *AIAA J* 29(5):784–790
- Amabili M, Karazis K, Khorshidi K (2011) Nonlinear vibrations of rectangular laminated composite plates with different boundary conditions. *Int J Struct Stab Dyn* 11(04):673–695
- Khorshidi K (2010) Analytical nonlinear elasto-plastic impact response of a moderately thick rectangular plate
- Yazdi AA (2013) Homotopy perturbation method for nonlinear vibration analysis of functionally graded plate. *J Vibr Acoustics*. <https://doi.org/10.1115/1.4023252>
- Quan TQ, Dinh Duc N (2016) Nonlinear vibration and dynamic response of shear deformable imperfect functionally graded double-curved shallow shells resting on elastic foundations in thermal environments. *J Thermal Stress* 39(4):437–459
- Quan TQ et al (2020) Vibration and nonlinear dynamic response of imperfect sandwich piezoelectric auxetic plate. *Mech Adv Mater Struct*. <https://doi.org/10.1080/15376494.2020.1752864>
- Andrianov I, Danishevs'Kyy V, Awrejcewicz J (2005) An artificial small perturbation parameter and nonlinear plate vibrations. *J Sound Vib* 283(3–5):561–571
- Duc ND, Van Tung H (2010) Nonlinear analysis of stability for functionally graded cylindrical panels under axial compression. *Comput Mater Sci* 49(4):S313–S316
- Quan TQ, Van Quyen N, Duc ND (2021) An analytical approach for nonlinear thermo-electro-elastic forced vibration of piezoelectric penta-Graphene plates. *Eur J Mech-A/Solids* 85:104095
- Li J-J, Cheng C-J (2005) Differential quadrature method for nonlinear vibration of orthotropic plates with finite deformation and transverse shear effect. *J Sound Vib* 281(1–2):295–309
- Lal A, Singh B, Kumar R (2008) Nonlinear free vibration of laminated composite plates on elastic foundation with random system properties. *Int J Mech Sci* 50(7):1203–1212
- Khoa ND, Thiem HT, Duc ND (2019) Nonlinear buckling and postbuckling of imperfect piezoelectric S-FGM circular cylindrical shells with metal-ceramic-metal layers in thermal environment using Reddy's third-order shear deformation shell theory. *Mech Adv Mater Struct* 26(3):248–259
- Tian A, Ye R, Chen Y (2016) A new higher order analysis model for sandwich plates with flexible core. *J Compos Mater* 50(7):949–961
- Kolekar S et al (2019) Vibration controllability of sandwich structures with smart materials of electrorheological fluids and magnetorheological materials: a review. *J Vibr Eng Technol*. <https://doi.org/10.1007/s42417-019-00120-5>
- Duc ND et al (2016) Nonlinear stability of eccentrically stiffened S-FGM elliptical cylindrical shells in thermal environment. *Thin-Walled Struct* 108:280–290
- Malekzadeh K et al (2006) Dynamic response of in-plane prestressed sandwich panels with a viscoelastic flexible core and different boundary conditions. *J Compos Mater* 40(16):1449–1469
- Nabarrete, A., A Three-Layer Quasi-3D Finite Element Analysis for Smart Actuation on Sandwich Plates. *Journal of Vibration Engineering & Technologies*, 2020: p. 1–11.
- Lv H et al (2021) The dynamic models, control strategies and applications for magnetorheological damping systems: a systematic review. *J Vibr Eng Technol* 9:131–147
- Duc ND (2016) Nonlinear thermal dynamic analysis of eccentrically stiffened S-FGM circular cylindrical shells surrounded on elastic foundations using the Reddy's third-order shear deformation shell theory. *Eur J Mech-A/Solids* 58:10–30
- Van Tung H, Duc ND (2010) Nonlinear analysis of stability for functionally graded plates under mechanical and thermal loads. *Compos Struct* 92(5):1184–1191
- Frostig Y, Thomsen OT (2004) High-order free vibration of sandwich panels with a flexible core. *Int J Solids Struct* 41(5–6):1697–1724
- Malekzadeh K, Khalili M, Mittal R (2005) Local and global damped vibrations of plates with a viscoelastic soft flexible core: an improved high-order approach. *J Sandwich Struct Mater* 7(5):431–456
- Carlson JD (2002) What makes a good MR fluid? *Electrorheological fluids and magnetorheological suspensions*. World Scientific, pp 63–69
- Yeh J-Y, Chen L-W (2004) Vibration of a sandwich plate with a constrained layer and electrorheological fluid core. *Compos Struct* 65(2):251–258

28. Yeh J-Y, Chen L-W (2007) Finite element dynamic analysis of orthotropic sandwich plates with an electrorheological fluid core layer. *Compos Struct* 78(3):368–376
29. Yeh J-Y, Chen L-W (2006) Dynamic stability analysis of a rectangular orthotropic sandwich plate with an electrorheological fluid core. *Compos Struct* 72(1):33–41
30. Yeh J-Y (2007) Vibration analyses of the annular plate with electrorheological fluid damping treatment. *Finite Elem Anal Des* 43(11–12):965–974
31. Yeh J-Y et al (2009) Damping and vibration analysis of polar orthotropic annular plates with ER treatment. *J Sound Vib* 325(1–2):1–13
32. Yeh J-Y (2011) Free vibration analysis of rotating polar orthotropic annular plate with ER damping treatment. *Compos B Eng* 42(4):781–788
33. Keshavarzian M et al (2020) High-order analysis of linear vibrations of a moderately thick sandwich panel with an electrorheological core. *Mech Adv Compos Struct* 7:177–188
34. Don DL, Coulter JP (1995) An analytical and experimental investigation of electrorheological material based adaptive beam structures. *J Intell Mater Syst Struct* 6(6):846–853
35. Yalcintas M, Coulter JP (1995) Analytical modeling of electrorheological material based adaptive beams. *J Intell Mater Syst Struct* 6(4):488–497
36. Nayfeh A, Nayfeh J, Mook D (1992) On methods for continuous systems with quadratic and cubic nonlinearities. *Nonlinear Dyn* 3(2):145–162
37. Singh P, Sundararajan V, Das Y (1974) Large amplitude vibration of some moderately thick structural elements. *J Sound Vib* 36(3):375–387
38. Marguerre K (1938) Zur theorie der gekrümmten platte grosser formänderung. In *Proceedings of the 5th international congress for applied mechanics*. John Wiley, New York
39. Chien R-D, Chen C-S (2006) Nonlinear vibration of laminated plates on an elastic foundation. *Thin-walled Struct* 44(8):852–860

Publisher's Note Springer Nature remains neutral with regard to jurisdictional claims in published maps and institutional affiliations.